SURFACE SCIENCE

Interaction of oxygen with palladium deposited on a thin alumina film

Sh. Shaikhutdinov [a], M. Heemeier [a], J. Hoffmann [a], I. Meusel [a], B. Richter [a],
M. Bäumer [a,*], H. Kuhlenbeck [a], J. Libuda [a], H.-J. Freund [a], R. Oldman [b],
S.D. Jackson [c], C. Konvicka [d], M. Schmid [d], P. Varga [d]

[a] *Abteilung Chemische Physik, Fritz-Haber-Institut der Max-Planck-Gesellschaft, Faradayweg 4–6, D-14195 Berlin, Germany*
[b] *ICI Technology, The Heath, Runcorn, Cheshire WA7 4QD, UK*
[c] *Department of Chemistry, Glasgow University, Glasgow G12 8QQ, UK*
[d] *Institut für Allgemeine Physik, Technische Universität Wien, A-1040 Wien, Austria*

Abstract

The interaction of oxygen with Pd particles, vapor deposited onto a thin alumina film grown on a NiAl(1 1 0) substrate, was studied by STM, AES, LEED, XPS, TPD and molecular beam techniques. The results show that O_2 exposure at 400–500 K strongly influences the oxide support. We suggest that the oxygen atoms formed by dissociation on the Pd surface can diffuse through the alumina film and react with the NiAl substrate underneath the Pd particles, thus increasing the thickness of the oxide film. The surface oxygen inhibits hydrogen adsorption, and readily reacts with CO at 300–500 K. For large and crystalline Pd particles, the system exhibits adsorption–desorption properties which are very similar to those of the Pd(1 1 1) single crystal surface. The molecular beam and TPD experiments reveal that, at low coverage, CO adsorbs slightly stronger on the smaller Pd particles, with an adsorption energy difference of $\approx$5–7 kJ mol^{-1} for 1 and 3–5 nm Pd particles studied. © 2002 Elsevier Science B.V. All rights reserved.

Keywords: Palladium; Aluminum oxide; Oxidation; Carbon monoxide; Chemisorption

1. Introduction

The preparation of *well-defined* model systems is an important precondition for studies aiming at a detailed understanding of catalytic mechanisms at a molecular level. In this respect, metal particles deposited on oxide films under controllable con-ditions have proven to be suitable model systems for highly dispersed metal catalysts supported on oxides [1–6].

In the last few years, we have studied the adsorption properties of Pd particles deposited onto a thin well-ordered alumina film grown on NiAl(1 1 0) [5,6]. For the non-dissociative adsorption of CO on this system, it was shown that the preferential adsorption geometry strongly depends on the size and morphology of the Pd particles [6,7]. For example, on the smallest particles and at high coverages, a large fraction of the CO is

* Corresponding author. Tel.: +49-30-8413-4100/4220; fax: +49-30-8413-4101/4312.
  E-mail address: baeumer@fhi-berlin.mpg.de (M. Bäumer).

adsorbed in on-top sites, while it occupies more bridge and/or threefold hollow sites on the well-ordered facets of large particles.

A similar behaviour has been observed for ethene adsorption: the distribution of π- and di-σ-bonded ethene molecules depends on the surface roughness and particle size, with π-bonded ethene preferentially formed on small and rough particles [8]. Obviously, small metal aggregates expose a higher fraction of low-coordinated atoms, resulting in adsorption properties different from those obtained for large faceted crystallites.

The interaction of oxygen and hydrogen with Pd particles turned out to be more complicated, because these molecules can dissociate on Pd, including the possibility that the ad-atoms migrate into sub-surface regions (see Ref. [9] for H and introduction in Ref. [10] as well as [11–15] for O). Indeed, in our recent molecular beam study we observed a large oxygen uptake by Pd particles on a $Al_2O_3/NiAl(1 1 0)$ substrate at and above room temperature. The origin of this effect was unclear at that time. As a possible explanation, oxygen migration into the sub-surface region of Pd was invoked [10].

In order to get more insight into this phenomenon, we have carried out an extended study employing scanning tunneling microscopy (STM), Auger electron spectroscopy (AES), low-energy electron diffraction (LEED), high resolution photoelectron spectroscopy (PES), temperature programmed desorption (TPD) and molecular beam techniques. The results obtained provide a detailed picture of the interaction of oxygen with the model system $Pd/Al_2O_3/NiAl(1 1 0)$.

2. Experimental

The experiments have been performed in several UHV chambers (base pressures below 10^{-10} mbar). The details of each experimental setup have been described in previous papers [8,16]. All UHV chambers are equipped with LEED and AES (Omicron SPECTALEED in Berlin, two-grid ErLEED and an additional Physical Electronics CMA for AES in Vienna) and facilities for preparation of metal deposits on a thin alumina film. In order to combine the results obtained in different chambers, the same preparation recipes were used.

The thin alumina film (thickness: 5–6 Å [5,17]) was prepared by oxidation of the clean NiAl(1 1 0) surface at 550 K and annealing at $\approx$1150 K [17]. Palladium (99.99%, Goodfellow (measurements in Berlin); 99.95%, Heraeus (measurements in Vienna)) was deposited onto the alumina film using commercial evaporators (Focus EFM3). Typical Pd deposition rates were about 0.5 Å min^{-1}, as calibrated with a quartz microbalance (1 Å nominal thickness of Pd corresponds to 6.81×10^{14} atoms cm^{-2}). During deposition, the sample was biased with a retarding potential in order to prevent metal ions from being accelerated towards the sample and creating nucleation centers on the surface [18].

In all chambers, a directional gas doser was used for gas adsorption in order to minimize contamination of the vacuum chamber. O_2 (99.999%), CO (99.99%) and deuterium (99.9%, isotopic content 99.5%) were supplied by AGA Gas (in Berlin) and Messer (in Vienna), respectively.

TPD spectra were measured in Berlin with a quadrupole mass spectrometer (QMS, Fisons). The mass spectrometer had a differentially pumped shield with an aperture of $\approx$6 mm. The nozzle of the shield was placed about 0.5 mm in front of the sample surface to minimize contributions originating from the sample heating wires. A linear temperature ramp with a heating rate of 5 K s^{-1} was generated using a feedback control system (Schlichting Physikalische Instrumente).

Details of the molecular beam experiments carried out in Berlin are given elsewhere [10,16]. Briefly, for the sticking coefficient measurements, an O_2 beam was generated from a supersonic expansion of O_2 at 300 K and a backing pressure of typically 1 bar. The supersonic beam intensity was of $\sim 2 \times 10^{13}$ molecules cm^{-2} s^{-1} for O_2 sticking coefficient experiments and $\sim 6 \times 10^{14}$ molecules cm^{-2} s^{-1} for CO experiments, respectively. The angle of incidence with respect to the surface normal was 35°.

The photoelectron spectra were recorded at the U49/1-PGM beamline at the BESSY II storage ring in Berlin with a 200 mm hemispherical energy analyzer (Scienta SES200). For the three photon

energies employed in the present study, the overall energy resolutions of the spectra (monochromator plus electron energy analyzer) were set to 30 meV for $E_{photon} = 150$ eV, 60 meV for $E_{photon} = 420$ eV and 90 meV for $E_{photon} = 640$ eV.

The STM data were obtained in Vienna in a two-chamber UHV system with a customized Omicron Micro-STM, using electrochemically etched and sputter-cleaned W tips. XPS results obtained in the same chamber with a laboratory XPS system (VG 300 W Mg Kα source, Specs EA10+ hemispherical analyzer) agree with the BESSY PES data, confirming that the sample preparations in the different labs were equivalent.

3. Results and discussion

3.1. Morphology

The morphology of the pristine Pd/Al$_2$O$_3$/NiAl(1 1 0) surface has already been studied in detail previously [5,8,19]. Briefly, the particles deposited at ∼90 K are uniformly distributed on the support due to preferential nucleation at point defects of the film [19]. In contrast to that, Pd deposited at room temperature nucleates at domain boundaries and steps of the alumina substrate and forms metal aggregates exposing mainly (1 1 1) facets [20].

The particle size gradually increases with increasing nominal thickness of the Pd overlayer [6]. The mean particle size can be determined from the particle density and the amount of Pd deposited assuming a hemispherical shape of the particles, for simplicity. The corresponding relationship between particle size and Pd nominal thickness has been presented in Ref. [8].

In order to investigate the influence of oxygen treatments at elevated temperatures on the surface morphology, STM measurements have been carried out. Fig. 1 shows images obtained for Pd crystallites (nominal thickness: 4 Å) grown at 300 K (a) and exposed to 300 L of oxygen at 400 K (b, c) and 480 K (d), respectively.

Turning to the results for the 400 K treatment first, a comparison between the two large scale images (a) and (b) reveals that the morphology
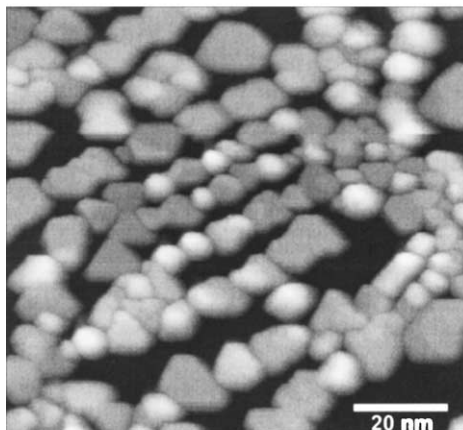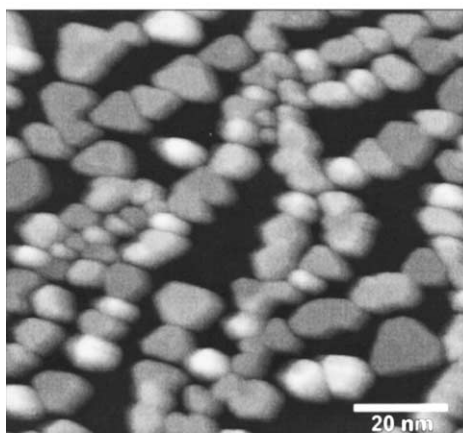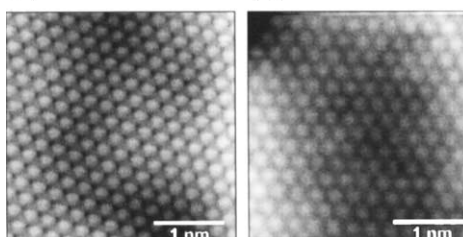
Fig. 1. STM images of Pd crystallites grown at 300 K (a) and treated with 300 L of oxygen at 400 K (b, c) and 480 K (d). (In the case of the experiment at 400 K, oxygen was supplied in three cycles of 100 L each. In the case of the experiment at 480 K, the whole dose was supplied at once, but the sample was already pretreated with 1200 L O$_2$ at 400 K.) The close-ups (c) and (d) show atomic resolution on the top facet of the crystallites. Tunneling parameters: $U_{sample} = -1.0$ V, 0.66 nA (a), $U_{sample} = -0.9$ V, 0.63 nA (b), $U_{sample} = -0.5$ mV, 7.1 nA (c), $U_{sample} = -0.5$ mV, 0.46 nA (d).

and the distribution of particles on the surface remains essentially unchanged after oxygen exposure. Also the uncovered parts of the support have a similar appearance. As demonstrated by the close-up of a single crystallite (c), it has been possible to obtain atomic resolution on the top layer of the Pd aggregates. In agreement with the untreated system (cf. Ref. [20]), we find a (1 1 1) orientation of the top layer. We could not observe any oxygen superstructure on the crystallites. This does not exclude the possibility of an ordered oxygen overlayer, such as a $p(2 \times 2)$ structure. We found that this structure is difficult to see and sometimes completely invisible on Pd(1 1 1) single crystals, presumably due to the high mobility of the oxygen atoms at room temperature. We can, however, definitely exclude the formation of an incommensurate structure of the kind found after high-dose oxidation at elevated temperatures (possibly a type of surface oxide) [25], since this structure leads to a rearrangement of the Pd atoms.

In Fig. 1d, an example of an atomically resolved crystallite after exposure to O_2 at 480 K is presented. Also in this case, the (1 1 1) orientation of the top facet is clearly visible allowing the conclusion that the particle morphology is also preserved under these conditions.

However, at this temperature and, in particular, at even higher temperatures, somewhat rounder particle shapes (cf. Ref. [10]) and increased particle heights were sometimes observed. Concomitantly, we experienced increasing difficulties due to unstable tunneling conditions (e.g. frequent tip crashes) during the STM measurements. In fact, reasonable images could only be obtained at relatively high voltages (>5 V) and low tunneling currents. This led to the suspicion of a significantly diminished conductivity of the oxygen treated samples. The origin of this effect, also supported by STM spectroscopy measurements, will become evident in the next sections.

3.2. Oxygen uptake

In order to measure the oxygen uptake of the Pd particles, we have performed sticking coefficient measurements of the King and Wells type
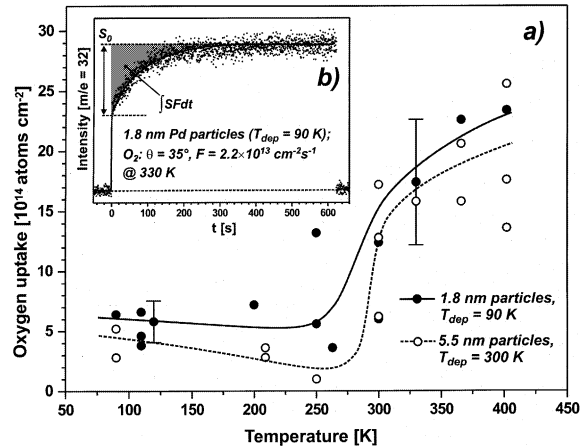
Fig. 2. (a) Oxygen uptake of the $Pd/Al_2O_3/NiAl(1\,1\,0)$ system as a function of temperature as determined from sticking coefficient measurements for two different samples exposed to 40 L of O_2. Open symbols: 5.5 nm particles prepared at 300 K (Pd surface atom density: 5.4×10^{14} cm^{-2}); filled symbols: 1.8 nm particles grown at 90 K. (b) Typical molecular beam measurement; the uptake is derived by integration of the shaded area.

[21,22] using molecular beam techniques. As depicted in Fig. 2, at $t = 0$ the O_2 beam is admitted to the scattering chamber, and the O_2 partial pressure is measured. The sticking coefficient S is directly determined from the reduced O_2 partial pressure with respect to the partial pressure at $S = 0$. The total oxygen uptake is derived by integration of the sticking coefficient S at known beam flux F as indicated in Fig. 2b. Typically, after exposures larger than approximately 20 L the sticking coefficient drops below the detection limit of the experiment (~ 0.02). Therefore, we have limited the O_2 exposures in *these* experiments to 40 L.

The measured values of oxygen uptake for two different samples, i.e. 1.8 nm particles prepared at 90 K (nominal thickness: 1 Å) and 5.5 nm particles prepared at 300 K (nominal thickness: 4 Å), are displayed in Fig. 2a. For the latter sample, exhibiting well-ordered (1 1 1) facets [6,10,23], the oxygen uptake per Pd surface atom is found to be 0.7 ± 0.2 at temperatures around 100 K. This value is close to the value of 0.62 obtained for mainly molecular oxygen adsorption on a Pd(1 1 1) single crystal surface [24]. With the temperature increasing to ~ 250 K, the saturation coverage decreases to ~ 0.2, as shown in Fig. 2a. This is again

consistent with the behaviour observed for the Pd(1 1 1) surface where the saturation coverage corresponds to 0.25 ML resulting in a p(2 × 2) superstructure.

On the smaller aggregates prepared at 90 K, the oxygen uptake appears to be slightly larger and the temperature dependence is less pronounced. This may be related to the higher defect density of the particle surface in this case [5,6].

Nevertheless, for both samples, Fig. 2a shows that the oxygen uptake drastically increases at temperatures above 250 K. At ∼400 K, the O coverage reaches values of approximately four O atoms per Pd surface atom. Thus, the uptake is an order of magnitude higher than the saturation coverage of a Pd(1 1 1) single crystal surface at these temperatures [25]. This finding strongly points to diffusion processes during oxygen exposure, which may involve either oxygen diffusion into the Pd particles, as observed for Pd single crystal surfaces and polycrystalline samples [11–15], and/or diffusion of adsorbed oxygen species into the alumina support.

3.3. Effect of the oxygen uptake: PES and AES studies

In order to identify, whether the oxygen uptake is related to oxygen diffusion into the bulk of the Pd particles or into the support, we have per-formed PES measurements of the 5.5 nm particles deposited at 300 K. The corresponding spectra of the Al 2p, Pd 3d and O 1s energy regions obtained at normal ($\theta = 0°$) and grazing ($\theta = 70°$) emission angles are shown in Fig. 3.

For the pristine Pd/Al$_2$O$_3$/NiAl sample, three components are observed in the Al 2p region (Fig. 3a). Previously, the signals at binding energy (BE) of 72.5, 73.6 and 74.8 eV (Al 2p$_{3/2}$) have been assigned to the Al atoms located in the NiAl(1 1 0) bulk, at the oxide–substrate interface and in the Al$_2$O$_3$ phase, respectively [5,17]. In the Pd 3d region, the bulk (marked b) and the surface (marked s) components of the Pd particles cannot be resolved due to the small surface core level shift (SCLS) of Pd(1 1 1) [26]. Finally, an O 1s peak centered at 531.3 eV with a shoulder at higher BE is characteristic for the pristine system.

After the sample is exposed to ∼1500 L of O$_2$ at 100 K (Fig. 3b), we observe a noticeable shift of the Pd 3d surface component to higher BE induced by the dense oxygen adsorbate layer formed in this temperature regime. Simultaneously, an additional emission feature on the high BE side of the O 1s peak (∼534 eV BE) is detected. Meanwhile, no drastic changes are observed in the Al 2p region.

Upon heating to 200 K (Fig. 3c), molecularly adsorbed oxygen partly dissociates and desorbs on Pd and the saturation coverage decreases [13] (see Fig. 2). In the photoelectron spectra, this change
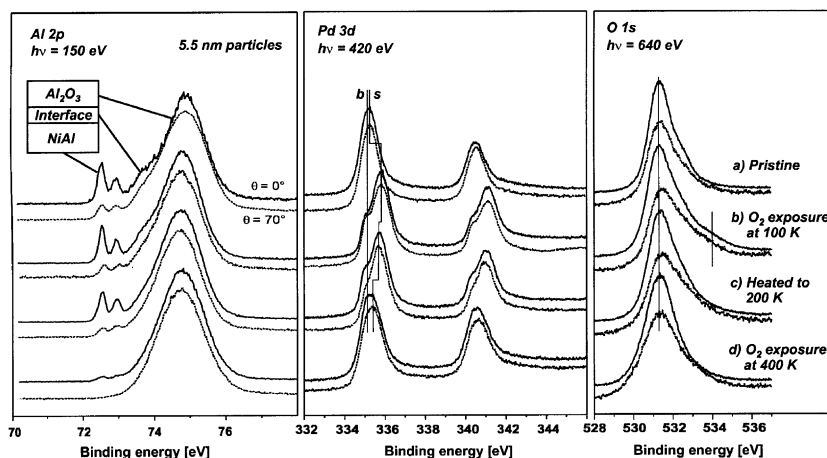
Fig. 3. Photoelectron spectra (Al 2p, Pd 3d, and O 1s regions) for Pd/Al$_2$O$_3$/NiAl(1 1 0) (particle size: 5.5 nm, T_{dep} = 300 K): freshly prepared (a); exposed to 1500 L of O$_2$ at 100 K (b) and then heated up to 200 K (c); after further exposure to 3000 L of O$_2$ at 400 K (d).

leads to a slight shift of the Pd surface component to lower BE with respect to the case of preferential molecular oxygen adsorption (cf. c and b). Simultaneously, the high BE feature in the O 1s region disappears.

Finally, we have inspected the sample after further exposure to 3000 L of O_2 at 400 K. The oxygen uptake measurements discussed above have shown that under these conditions the system incorporates large amounts of oxygen. However, the changes in the Pd 3d signal turn out to be quite moderate as shown in Fig. 3d. The Pd surface component is found to be further shifted back to lower BE, which is consistent with the reduced oxygen saturation coverage observed on Pd surfaces at elevated adsorption temperatures [24]. From these results, the extent to which oxygen is dissolved in the Pd particles cannot be quantified. However, the formation of a PdO-like phase can definitely be excluded on the basis of a comparative XPS study of Pd and PdO [27].

The most drastic effect, however, is observed in the Al 2p region. The signals corresponding to Al atoms in the NiAl bulk and the interface regions are strongly attenuated, indicating that the *oxide film thickness* increases significantly under these conditions.

In order to get an estimate of the thickness of the additional oxide layer formed during the oxygen treatment, we have determined the intensity ratios of the Al 2p peaks originating from NiAl and Al_2O_3 for a series of spectra recorded at different photon energies between 150 and 950 eV and at detection angles between 0° and 60°. From the attenuation of the NiAl component and the electron inelastic mean free paths in Al_2O_3 [28], the increase in the overlayer thickness may be calculated. (Note that the thickness of the pristine film corresponds to roughly 5 Å [5].) Assuming a spatially homogeneous oxide film growth, we estimate that an *additional* oxide layer of 9.5 ± 2 Å thickness is formed when exposing the system Pd/Al_2O_3/NiAl(1 1 0) to O_2 at 400 K. This value would correspond to 3–5 extra layers of oxygen. As the attenuation will be weaker for a non-homogeneous layer, this value may be considered as a lower limit for the amount of oxide additionally formed.

It is worth noting in this context that the observed increase in the oxide thickness would require an oxygen uptake of $(5 \pm 1) \times 10^{15}$ atoms cm^{-2}. Since this value exceeds the uptake determined in the sticking coefficient measurements shown in Fig. 2 ($\sim 2 \times 10^{15}$ atoms cm^{-2}), we can conclude that the oxidation process proceeds at a slow rate even after the sticking probability has dropped below the detection limit of the molecular beam experiment, i.e. after an exposure to 40 L of oxygen. Thus, in order to reach full saturation of the system, this exposure is not sufficient and higher doses, probably in the order of 10^2–10^3 L, are needed.

The thickening of the oxide film has also been confirmed for Pd particles grown at 90 K using Auger spectroscopy. Here, the oxygen treatment was carried out at 400 and 500 K in order to check the effect of higher oxidation temperatures as well. (In these experiments, surface oxygen was removed by exposure to CO and subsequent heating to 600 K: see Section 3.5).

Fig. 4 shows peak-to-peak heights of the Pd (330 eV), O (510 eV) and Ni (848 eV) AES signals
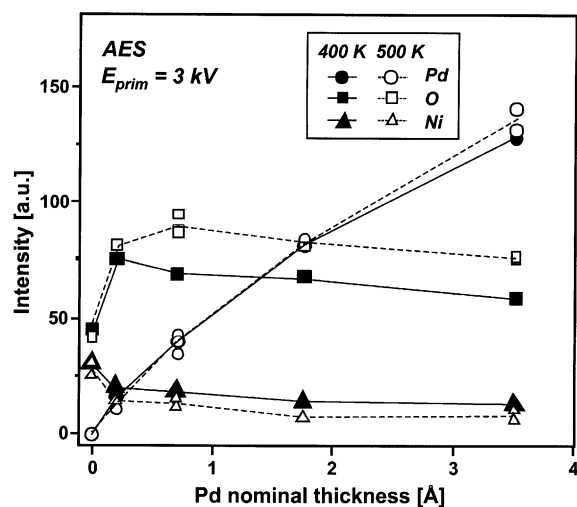
Fig. 4. Intensities of Pd (330 eV), O (510 eV) and Ni (848 eV) AES peaks for Pd particles grown at 90 K and treated with oxygen (500 L) at 400 K (filled symbol, solid lines) and 500 K (open symbol, dotted lines) as a function of the Pd nominal thickness. In order to remove surface oxygen from Pd, the samples were exposed to 4 L CO at 300 K and heated to 600 K prior to measurements.

as a function of Pd nominal thickness. As expected, the Pd signal increases and the Ni signal decreases with increasing Pd coverage. Meanwhile, the O signal strongly increases for coverages below 0.3 Å and slightly decreases above ∼1 Å . Such a behaviour is opposite to that observed for the pristine samples, where the AES intensities of the substrate elements, such as Al, Ni and O, gradually decrease as the Pd coverage increases. It is interesting to note that, in all cases, the intensity of the oxygen peak is even higher than on the Pd-free alumina film. The AES results are thus in agreement with the PES data, i.e. additional oxide layers are formed in the case of the 90 K deposits as well.

Raising the oxidation temperature from 400 to 500 K leads to even larger O signals, while the Ni signal is further suppressed. Apparently, higher temperatures result in larger oxygen uptakes, i.e. thicker oxide films.

3.4. Effect on the support: LEED study

The Al_2O_3/NiAl(1 1 0) surface exhibits a comparatively complex LEED pattern which is described in detail elsewhere [5]. The large number of diffraction spots, observed in addition to the NiAl substrate spots, is the result of the *specific* long-range order of the alumina film featuring an exceptionally large unit cell. Due to the twofold symmetry of the NiAl(1 1 0) surface, the film grows in two reflection domains.

The diagram presented in Fig. 5 shows how the intensities of the alumina and NiAl substrate diffraction spots change depending on the treatment applied. Deposition of 4 Å Pd at 300 K attenuates the intensity of the oxide superstructure by ∼40%. Annealing at 400 K for 15 min does not result in any further changes (not shown), while oxygen exposure (200 L) at the same temperature for 15 min decreases the intensity further by a factor of 2. The intensity does not change after exposure to CO removing surface oxygen from the Pd particles (see Section 3.5).

On the basis of these results, it can be concluded that the oxygen treatment modifies the specific long-range order of the alumina film. Notably, this is only the case in the presence of Pd. Oxygen
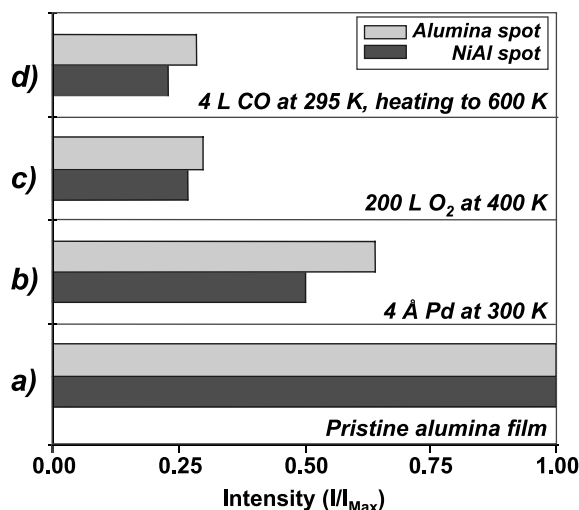
Fig. 5. The diagram shows relative LEED intensities of the alumina film and the NiAl substrate ($E_0 = 65$ eV) as recorded after the following preparation steps: (a) pristine system; (b) subsequent deposition of Pd with a nominal thickness of 4 Å at 300 K (particle size: 5.5 nm); (c) exposure of this system to 200 L oxygen at 400 K; (d) followed by an exposure to 4 L CO at room temperature and annealing to 600 K.

exposure of the Pd-free, clean film leads to no changes of the LEED pattern.

Apart from the superstructure spots, the beams originating from the NiAl substrate are strongly attenuated. This is in agreement with the PES data and can readily be explained by the thickening of the alumina film.

Note that particles prepared at 300 K preferentially decorate line defects so that a significant fraction of the support remains uncovered (see Fig. 1). More dramatic changes occur for samples prepared at 90 K where particle densities are up to an order of magnitude higher than at 300 K [6]. Starting from a Pd nominal thickness of 0.2 Å, a LEED pattern could not be detected at all after an oxygen exposure at 400–500 K. Obviously, the higher density of particles obtained at low temperatures due to nucleation at point defects and their random distribution on the surface result in even larger modifications of the support.

In summary, the LEED data reveal that, although the thickness of the oxide film increases, the specific structure of the original film is affected.

Also, no indications of new diffraction spots have been observed so that the formation of a new long-range order seems unlikely.

3.5. Effect on the Pd deposits: TPD study

Although the largest fraction of oxygen is apparently consumed by the reaction with the NiAl substrate, chemisorbed oxygen is still present on the surface of the particles after the oxygen treatment. This has been evidenced by its reaction with CO in molecular beam experiments [10]. In addition to that, multi-mass TPD recorded after adsorption of CO (4 L) at room temperature revealed the formation of CO_2 desorbing in a broad signal between 300 and 500 K due to the recombination of CO and O. The integral intensity of the CO_2 signal basically follows the Pd coverage. Note that no further CO_2 was detected in subsequent TPD runs, indicating that the "reduction" step removes surface oxygen completely.

The presence of oxygen manifests itself also in the hydrogen adsorption behaviour of the pretreated particles. The spectra in Fig. 6 represent typical D_2 TPD traces recorded for samples freshly prepared at 90 K and heated to 380 K (to remove hydrogen adsorbed from the vacuum background). These surfaces were subsequently ex-

posed to 500 L of O_2 at 500 K and then "reduced" by exposure to CO at 300 K and heating to 600 K. Two desorption peaks are visible at ∼350 and ∼240 K which have previously been assigned to hydrogen atoms residing on the surface and to species presumably in sub-surface sites, respectively [8].

When comparing the spectra (1) and (2), it becomes evident that hydrogen adsorption on the surface is suppressed on the pretreated system. This can be understood in terms of a site-blocking effect due to the oxygen ad-atoms. As a result, the amount of water D_2O expected due to the O + D reaction is negligible. Those D atoms, which nevertheless adsorb, are weakly bound and probably occupy sub-surface sites.

Removal of the surface oxygen with CO renders the hydrogen chemisorption possible again and the D_2 TPD spectrum is basically restored (cf. spectra 1 and 3 in Fig. 6). In particular, the intensity of the peak at 350 K, corresponding to surface hydrogen, is nearly the same as for a pristine sample. This indicates that the Pd surface area is not much influenced by the treatments applied. The low temperature desorption peak (sub-surface hydrogen), however, gains intensity. This raises the question whether some oxygen is dissolved in the bulk of the Pd particles, possibly influencing the adsorption (and reaction) properties. However, no water formation is detected via TPD as might be expected from the reaction of sub-surface hydrogen and sub-surface oxygen.

In this context, also a molecular beam study regarding the CO oxidation reaction on the oxygen pretreated $Pd/Al_2O_3/NiAl(1\,1\,0)$ system is worth mentioning [10,23]. Experiments on large (5.5 nm) well-faceted Pd particles provided activation energies for the Langmuir–Hinshelwood (LH) step of the reaction of 57 ± 6 and 62 ± 8 kJ mol^{-1} for CO and O precovered surfaces, respectively. These values agree well with the activation energies obtained for the Pd(1 1 1) single crystal surface under high coverage conditions (59 ± 8 kJ mol^{-1} [29,30]). Therefore, at least for the large (1 1 1)-oriented Pd particles, the LH activation energies are not affected by the oxygen pretreatment, i.e. the reaction kinetics approach the Pd(1 1 1) single crystal behaviour.
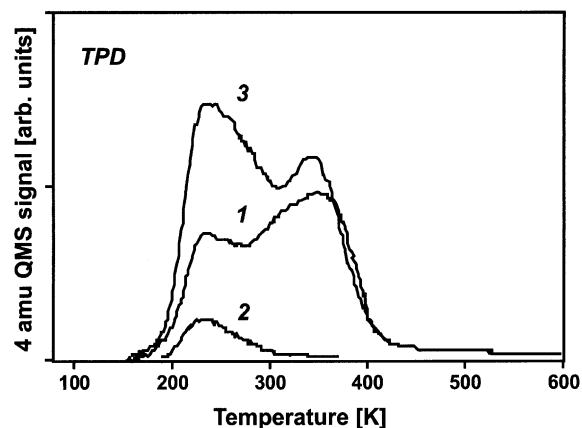
Fig. 6. TPD spectra for Pd particles (size: 1.4 nm) deposited at 90 K, flashed in vacuum to 380 K (1), exposed to 500 L of O_2 at 500 K (2); then exposed to 4 L of CO at 295 K and heated up to 600 K (3). For each TPD run, the sample was exposed to 2 L of D_2 at 195 K.

3.6. CO adsorption/desorption behaviour of the oxygen treated system

Fig. 7 summarizes the results of a molecular beam study of CO interaction with the "reduced" system. The surface was exposed to a modulated CO beam, and the CO background pressure was synchronously recorded. In the CO signals shown in Fig. 7a (deconvoluted to correct for the finite pumping speed in the scattering chamber), the
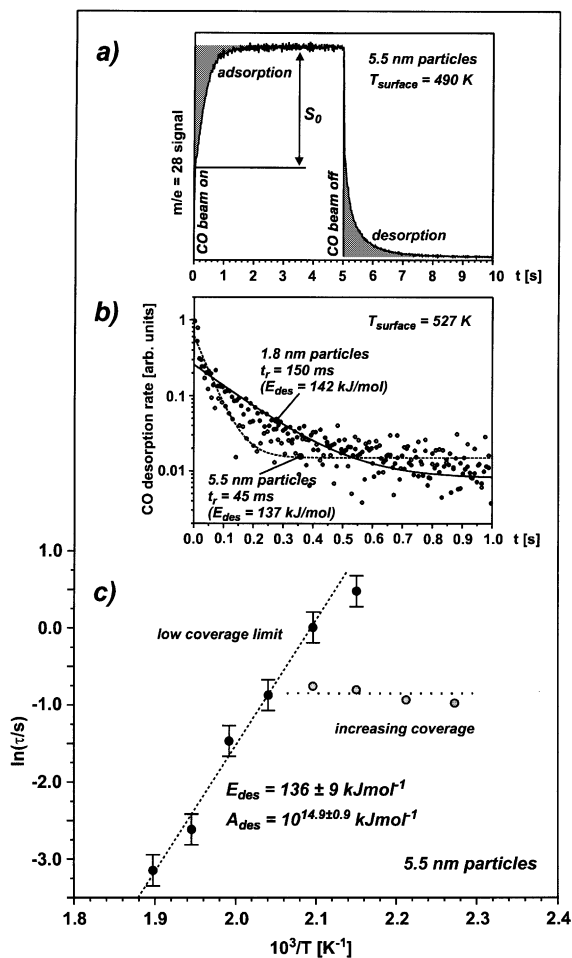
Fig. 7. (a) CO residence time measurement on oxygen pretreated Pd/Al$_2$O$_3$/NiAl(1 1 0) using a modulated CO beam; (b) CO surface residence times on oxygen pretreated Pd/Al$_2$O$_3$/ NiAl(1 1 0) for two types of Pd particles; (c) determination of the activation energy and pre-exponential factor for desorption of CO from oxygen pretreated Pd/Al$_2$O$_3$/NiAl(1 1 0) (see text for details).

rapid response due to direct scattering and adsorption/desorption from the inert support can be clearly distinguished from the slower response originating from adsorption/desorption from the Pd particles. By analyzing the relatively slow tail on the desorption rate (see Fig. 7b), we can measure the CO residence time on the particles. From the temperature dependence of the residence time, the activation energy and the pre-exponential factor for CO desorption can be determined as shown in Fig. 7c.

It should be noted, however, that the desorption rates show a single exponential decay only in the low coverage regime. With increasing CO coverage, the repulsive interaction between neighbouring CO molecules leads to increasing desorption rates (see Fig. 7c). Therefore, we limit the determination of the desorption energy to low coverages only, where a value of 136 ± 9 kJ mol^{-1} and a pre-exponential factor of $10^{14.9 \pm 0.9}$ s^{-1} are calculated for the 5.5 nm Pd particles. These values are in good agreement with those obtained for a Pd(1 1 1) single crystal, i.e., 134 ± 8 kJ mol^{-1}, $10^{14.4 \pm 0.8}$ s^{-1} [30]. This again indicates that the adsorption/desorption behaviour of the large well-faceted Pd particles approaches the behaviour of the Pd(1 1 1) single crystal.

It is noteworthy that slightly increased residence times have been observed for smaller particles in the low coverage limit (see Fig. 7b). The measured increase in the residence time corresponds to an increase in the desorption energy of approximately 5 kJ mol^{-1}, assuming identical pre-exponential factors.

In order to further study particle size effects in the CO interaction with Pd, we have performed TPD measurements with different Pd coverages. To this end, Pd was deposited at 90 K, followed by exposure to 500 L of O$_2$ at 500 K. Then, samples were exposed to 4 L of CO at 300 K and heated up to 600 K. The reduced samples were exposed to 2 L of CO at 100 K prior to a TPD run.

Fig. 8 shows a family of CO TPD spectra as a function of the particle size. The spectra are very reproducible so that morphological changes during TPD runs up to ∼600 K can be excluded.

Two desorption features can be distinguished in the spectra: a broad signal at low temperature
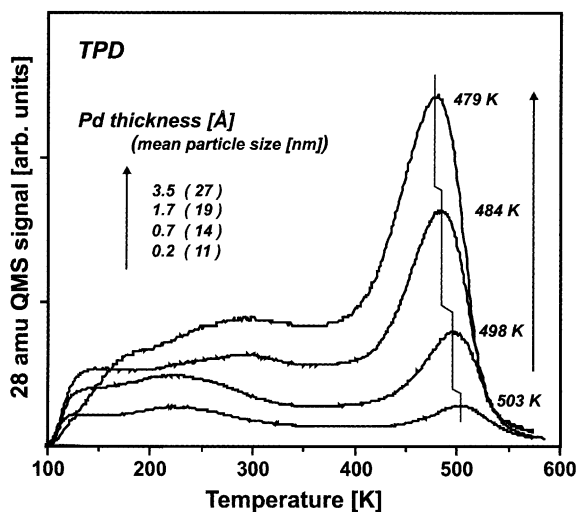
Fig. 8. CO TPD spectra for Pd particles ($T_{dep} = 90$ K) pre-treated with oxygen at 500 K and reduced with CO as a function of particle size. Samples were exposed to 2 L of CO at 100 K in each case.

(LT) and a high temperature (HT) peak centered at ∼500 K. On the basis of infrared spectroscopy and TPD studies of CO adsorbed on Pd particles [5–7,18], these states may be attributed to CO desorbing from on-top and multiply coordinated (basically threefold hollow) sites, respectively.

Starting from low temperature, CO desorbs from the on-top sites first. As the coverage decreases, the remaining CO molecules occupy the more favourable highly coordinated sites from which they desorb at a higher temperature. Comparing the TPD spectra for different Pd coverages (Fig. 8), it is obvious that the site occupation is strongly particle size dependent (cf. Ref. [6]). The increasing intensity of the LT signal as compared to the HT signal implies a preference for on-top adsorption on small particles. This behaviour is in line with that observed for the pristine Pd particles [5,6], again corroborating the similar adsorption properties of the pristine and pretreated Pd/Al$_2$O$_3$/NiAl(1 1 0) system.

Another particle size effect reveals itself in the gradual shift of the HT peak to lower temperatures with increasing particle size. This indicates that CO, in the *low coverage regime*, adsorbs more strongly on the smaller particles. The shift of about 25 K in desorption temperature corresponds

to an adsorption energy difference of about 7 kJ mol^{-1} for ∼1 and ∼3 nm particles studied. This value is in good agreement with 5 kJ mol^{-1} found by the CO residence time measurements for 1.8 and 5.5 nm particles, as shown in Fig. 7b.

4. Summary and conclusions

Finally, we would like to summarize the results found by a combined STM, AES, LEED, PES, TPD and molecular beam study for the system Pd/Al$_2$O$_3$/NiAl(1 1 0).

During oxygen exposure at 400–500 K, oxygen molecules readily dissociate on Pd. Oxygen is consumed in amounts significantly exceeding the saturation coverage of the Pd deposits. No bulk Pd oxide phases are formed, as found by PES.

The oxygen atoms on the Pd surface can react with adsorbed CO molecules and form CO$_2$, with both molecules desorbing upon heating to 550 K. No CO$_2$ production is found after subsequent CO exposures. In the same way, no water is formed after hydrogen adsorption.

Changes are observed for the alumina substrate. According to AES and PES studies, the thickness of the oxide film is drastically increased, on average, by 3–5 additional sub-layers of oxygen at 400 K. On raising the temperature, even thicker films can be obtained. Concomitantly, the film loses its specific long-range order, as judged by LEED, but no additional surface roughness is observed by STM. In the case of the well-faceted aggregates grown at 300 K and treated at 400 K, there are also no indications that the particle morphology is affected. After oxygen treatments at higher temperatures, the STM data sometimes imply somewhat rounder particle shapes as well as increased particle heights. The extent to which this reflects morphological changes, however, is not clear. Apart from geometrical effects, electronic effects, connected with the limited conductivity of the thicker films for instance, could play a role.

Accordingly, the data suggest that the largest fraction of the oxygen atoms migrates into the substrate during oxygen exposures at elevated temperatures. However, the formation of certain
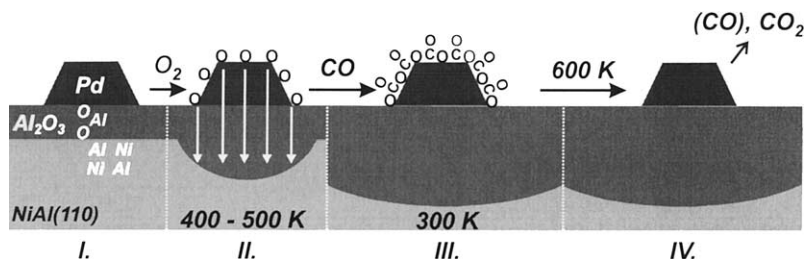
Fig. 9. The proposed mechanism for the interaction of Pd particles deposited on Al_2O_3/NiAl(1 1 0) with O_2 at elevated temperatures. It involves dissociation of oxygen on Pd, its diffusion through the oxide film and reaction with the metallic substrate underneath (II). At temperatures above 400 K, the oxide film becomes thicker by about 3–5 oxygen sub-layers. Surface oxygen reacts with CO during the reduction step (III), followed by CO and CO_2 desorption upon heating to 600 K (IV). The resulting surface exhibits adsorption–desorption properties very similar to the pristine samples.

amounts of sub-surface and bulk oxygen in Pd, as reported in other cases [11–15], cannot be completely excluded at this point. The resulting system exhibits adsorption properties essentially identical to the metallic Pd surface with respect to CO and hydrogen.

On the basis of these results, we propose a possible *scenario* of the processes taking place during the oxygen treatment. This is depicted in Fig. 9. Molecular oxygen dissociates on Pd at $T > 250$ K. The oxygen atoms formed migrate through the alumina film below the Pd particles or at their periphery. The oxygen species can then react with the metallic NiAl substrate underneath. Such a process can be driven by the higher heat of formation for Al_2O_3 (-1678 kJ mol^{-1}) as compared to PdO (-113 kJ mol^{-1}) [31]. The migration of oxygen could proceed via sub-surface or bulk oxygen in Pd as intermediate states. However, further in situ experiments are necessary to prove this.

The increasing thickness of the oxide obviously suppresses the oxygen migration. Therefore, the atomic oxygen flow from Pd to the support declines. Finally, the oxygen ad-atoms reside on the Pd surface and therefore the O_2 sticking coefficient drops to zero.

Thus, we suggest that Pd acts as a catalyst for the oxidation of the metal substrate below the alumina film by supplying the reactive oxygen atoms formed during oxygen dissociation on Pd. A similar behaviour has recently been observed for vanadium deposited on the alumina film at elevated temperatures and in an ambient atmosphere of oxygen [32].

Probably, oxygen diffusion is the rate limiting step for such a process involving dissociation, migration and reaction stages. Since diffusion is enhanced at higher temperatures, the film becomes on average thicker at 500 K as compared with oxidation at 400 K.

The oxygen pretreated system clearly shows particle size effects in TPD and molecular beam experiments: in the low coverage regime, CO adsorbs more strongly on the smaller particles. However, the energy differences are rather small and correspond to 5–7 kJ mol^{-1} for particles sizes ranging between 1 and 5 nm. This observation is in line with the results of Chou and Vannice obtained on highly dispersed Pd/Al_2O_3 catalysts, showing that heat of CO adsorption increases for a particle size below 3 nm [33].

References

[1] C.R. Henry, Surf. Sci. Rep. 31 (1998) 231.
[2] D.W. Goodman, Surf. Rev. Lett. 2 (1995) 9.

[3] C.T. Campbell, Surf. Sci. Rep. 27 (1997) 1.

[4] H.-J. Freund, Angew. Chem. Int. Ed. Engl. 36 (1997) 452.

[5] M. Bäumer, H.-J. Freund, Prog. Surf. Sci. 61 (1999) 127.

[6] M. Frank, M. Bäumer, Phys. Chem. Chem. Phys. 2 (2000) 3723.

[7] K. Wolter, O. Seiferth, H. Kuhlenbeck, M. Bäumer, H.-J. Freund, Surf. Sci. 399 (1998) 190.

[8] Sh. Shaikhutdinov, M. Heemeier, M. Bäumer, T. Lear, D. Lennon, R.J. Oldman, S.D. Jackson, H.-J. Freund, J. Catal. 200 (2001) 330.

[9] Z. Paal, P.G. Menon (Eds.), Hydrogen Effects in Catalysis, Marcel Dekker, New York, 1988.

[10] I. Meusel, J. Hoffmann, J. Hartmann, M. Heemeier, M. Bäumer, J. Libuda, H.-J. Freund, Catal. Lett. 71 (2001) 5.

[11] F.P. Leisenberger, G. Koller, M. Sock, S. Surnev, M.G. Ramsey, F.P. Netzer, B. Klötzer, K. Hayek, Surf. Sci. 445 (2000) 380.

[12] V.A. Bondzie, P. Kleban, D.W. Dwyer, Surf. Sci. 347 (1996) 319.

[13] M. Milun, P. Pervan, K. Wandelt, Surf. Sci. 218 (1989) 363.

[14] M. Milun, P. Pervan, M. Vacjic, K. Wandelt, Surf. Sci. 211–212 (1989) 887.

[15] D.L. Weissman-Wenicur, M.L. Shek, P.M. Stefan, I. Lindau, W.E. Spicer, Surf. Sci. 127 (1983) 513.

[16] J. Libuda, I. Meusel, J. Hartmann, H.-J. Freund, Rev. Sci. Instrum. 71 (2000) 4395.

[17] R.M. Jaeger, H. Kuhlenbeck, H.-J. Freund, M. Wuttig, W. Hoffmann, R. Franchy, H. Ibach, Surf. Sci. 259 (1991) 235.

[18] J. Libuda, Ph.D. Thesis, Ruhr-Universität Bochum, 1996.

[19] M. Bäumer, M. Frank, M. Heemeier, R. Kühnemuth, S. Stempel, H.-J. Freund, Surf. Sci. 454/456 (2000) 957.

[20] K.H. Hansen, T. Worren, S. Stempel, E. Lægsgaard, M. Bäumer, H.-J. Freund, F. Besenbacher, I. Stensgaard, Phys. Rev. Lett. 83 (1999) 4120.

[21] D.A. King, M.G. Wells, Proc. Roy. Soc. London, Ser. A 339 (1974) 245.

[22] D.A. King, M.G. Wells, Surf. Sci. 29 (1972) 454.

[23] I. Meusel, J. Hoffmann, J. Hartmann, J. Libuda, H.-J. Freund, J. Phys. Chem. B 105 (2001) 3567.

[24] X. Guo, A. Hoffman, J.T. Yates Jr., J. Chem. Phys. 90 (1989) 5787.

[25] G. Zheng, E.I. Altman, Surf. Sci. 462 (2000) 151.

[26] J.N. Andersen, D. Hennig, E. Lundgren, M. Methfessel, R. Nyholm, M. Scheffler, Phys. Rev. B 50 (1994) 17525.

[27] M. Brun, A. Berthet, J.C. Bertolini, J. Electron Spectros. Relat. Phenom. 104 (1999) 55.

[28] S. Tanuma, C.J. Powell, D.R. Penn, Surf. Interf. Anal. 17 (1991) 927.

[29] T. Engel, G. Ertl, J. Chem. Phys. 69 (1978) 1267.

[30] T. Engel, J. Chem. Phys. 69 (1978) 323.

[31] D.R. Lide (Ed.), CRC Handbook of Chemistry and Physics, 72nd ed., CRC Press, Boca Raton, 1991–1992.

[32] M. Bäumer, J. Biener, R.J. Madix, Surf. Sci. 432 (1999) 189.

[33] P. Chou, A.M. Vannice, J. Catal. 104 (1987) 17.